

**FINAL TECHNICAL REPORT: 1990**

**Name of Grantee:** **University of Washington**

**Principal Investigator:** **R. S. Crosson  
K. C. Creager  
Geophysics Program AK-50  
University of Washington  
Seattle, WA 98195**

**Government Technical Officer:** **Dr. Elaine R. Padovani  
U. S. Geological Survey  
905 National Center  
Reston, VA 22092**

**Short Title:** **Earthquake Hazard Research in the Pacific Northwest**

**Effective Date of Grant:** **February 1, 1990**

**Grant Expiration Date:** **January 31, 1991**

**Amount of Grant:** **\$94,667.**

**Date Report Submitted:** **May 25, 1991**

**Sponsored by the  
U.S. Geological Survey  
Grant No. 14-08-0001-G1803**

**The contents of this report were developed under a grant from  
the U. S. Geological Survey, Department of the Interior. However,  
those contents do not necessarily represent the policy of that agency,  
and you should not assume endorsement by the Federal Government.**

## CONTENTS

Summary .....	1
Tomographic imaging .....	2
Slab Kinematics .....	4
Publications funded under this contract .....	11
Acknowledgements .....	11
References .....	11

## FIGURES

Figure 1: Perspective plot of upper mantle subducted slab .....	3
Figure 2: Fixed geometry ( $20^\circ$ dip everywhere) plate strain .....	6
a) Map view of orientation and magnitude of in-plane strain rate ( $s^{-1}$ )	
b) Map view of effective strain rate ( $s^{-1}$ )	
c) Map view of model geometry; depth contours	
Figure 3: Free geometry plate strain (dip constrained to $20^\circ$ only at ends of slab) .....	7
a) Map view of orientation and magnitude of in-plane strain rate ( $s^{-1}$ )	
b) Map view of effective strain rate ( $s^{-1}$ )	
c) Map view of model geometry; depth contours	
Figure 4: Comparison of arch from inversion with volcanic compositional data .....	8
a) Perspective view of arch model from Fig. 3	
b) Map view of model geometry from Fig. 3	
c) Plate depth from volcanic composition (from Dickinson, 1970)	
Figure 5: Strain effects of bending Gaussian arches.....	9
a) Strain associated with subduction of a uniform arch	
b) Strain associated with subduction of an arch which diminishes in height prior to bending	

## APPENDICES

1. Recent Abstracts
2. JGR reprint: Creager, K.C., and T.M. Boyd, The geometry of Aleutian subduction: three-dimensional kinematic flow model
3. U.S.G.S. Professional Paper Pre-print: Ma, Li, R.S. Crosson, and R.S. Ludwin, Preliminary Report on Focal Mechanisms and stress in western Washington
4. Extended Abstract: VanDecar, J.C., R.S. Crosson, and K.C. Creager, Teleseismic travel-time inversion for Cascadia subduction zone structure employing three-dimensional ray tracing

## Summary

This is the final technical report for USGS grant 14-08-0001-1803, "Earthquake Hazard Investigations in the Pacific Northwest" during the period 2/1/90 - 1/31/91. The objective of our research is to investigate earthquake hazards in the Pacific Northwest including problems related to possible large subduction earthquakes. Improvement in our understanding of earthquake hazards is based on better understanding of the regional structure and tectonics. A primary source of our data is the Washington Regional Seismograph Network (WRSN), and our studies require cooperation and collaboration between a number of individuals and projects. Current investigations by our research group focus on the configuration of the subducting Juan de Fuca plate, differences in characteristics of seismicity between the overlying North American and the subducting Juan de Fuca plates, and kinematic modeling of deformation of the subducting Juan de Fuca slab.

Appendix 1 contains copies of recent abstracts. Appendix 2 is a reprint of a JGR article entitled "The geometry of Aleutian subduction: three-dimensional kinematic flow model" by K.C. Creager and T.M. Boyd. Appendix 3 is a preprint of an article for the USGS Professional Paper (Assessing and Reducing Earthquake Hazards in the Pacific Northwest) entitled "Preliminary Report on Focal Mechanisms and stress in western Washington" by Li Ma, R.S. Crosson, and R.S. Ludwin. Appendix 4 is a preprint of an extended abstract which was presented at the XXII General Assembly of the European Seismological Commission, Barcelona, Spain, Fall 1990. The abstract is titled "Teleseismic travel-time inversion for Cascadia subduction zone structure employing three-dimensional ray tracing", by J.C. VanDecar, R.S. Crosson, and K.C. Creager.

We expect two students to complete Ph.D.s in 1991, one on upper mantle velocity structure from seismic tomography, the other on kinematic modeling. This report includes two sections, one on our work with tomographic imaging, and the other dealing with kinematic modeling.

### Tomographic imaging

Using an approximation to non-linear inversion, we estimated the velocity structure of the upper mantle portion of the Cascadia subduction zone using a data set of approximately 10,000 relative arrival times of teleseismic *P* waves recorded from 1980 to 1990 on the WRSN (Washington Regional Seismic Network) short-period vertical stations in Washington and Northern Oregon. To approximate non-linear inversion, linear travel-time inversions (conjugate gradient method) were performed alternately with three-dimensional ray tracing. Smoothing of the final model is achieved through an auxiliary set of constraint equations.

The most prominent and robust characteristic of the models obtained is a steeply eastward dipping fast, planar feature which is inferred to be the thermal and compositional anomaly associated with the subducting Juan de Fuca oceanic plate. The high velocity zone is located at a depth of approximately 100 km beneath the Cascade volcanos, similar to subduction zones elsewhere. At shallow depths (i.e. 60-80 km) the velocity anomaly is consistent with projections from models of slab structure from 40-60 km depth.

At 48° N latitude, the high velocity zone extends to depths of 400 km or more. However, south of 46°, the velocity anomaly disappears at a depth of ~ 150 km. Considering the relative plate motions, our interpretation is consistent with a deep slab which has separated completely from the shallow slab in the south, and descended into the mantle. Figure 1 shows a three-dimensional perspective plot of the volume of 1% higher velocity material interpreted as the subducted Juan de Fuca slab. The three-dimensional structure is used to model other geophysical observations such as the regional gravity field and *P*-wave amplitude variations due to geometrical ray spreading.

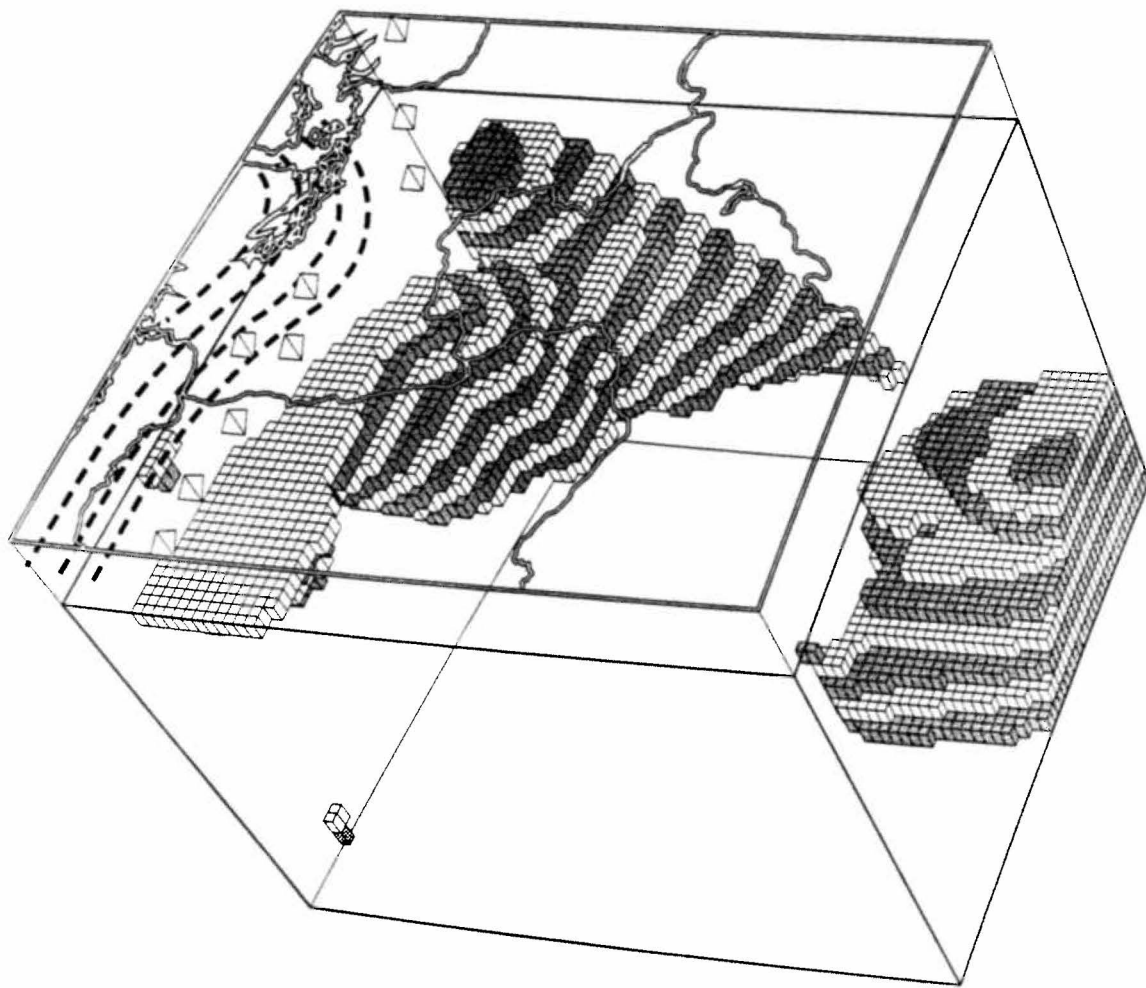


Figure 1. Compressional wave velocity model determined by non-linear inversion of teleseismic arrival times of 10,000 P and PKP waves. The region shown extends from 100 to 600 km in depth, from 44° to 50° north latitude, and from 114° to 124° west longitude. Outlines of Washington and Oregon are shown on the top surface of the box, and pyramids represent Quaternary strato-volcanos. Dashed contour lines indicate inferred depths (30, 40, 50 and 60 km) to shallow slab (Crosson and Owens, 1987). The shaded volume represents velocities exceeding the Herrin model by 1% or more. An anomaly beneath the Blue Mtns. of NE Oregon has been omitted for clarity.

### Kinematic modeling

The well-located microseismicity recorded by the WRSN during the past two decades is concentrated in the vicinity of the Puget Sound Basin. Combining this catalog with events greater than magnitude 6 during the last century, the distribution of seismic moment release of subcrustal events displays an even more pronounced concentration beneath the Puget Sound Basin, extending from Olympia, Washington to Victoria, British Columbia. Intra-slab moment release in this area is four orders of magnitude higher than background seismicity to the north and to the south. Based on seismicity and other evidence, the slab dips  $20^\circ$  under central Vancouver Island,  $10^\circ$  across the Olympic Peninsula Puget Sound area, and about  $20^\circ$  under Oregon, defining an arching slab geometry with the axis of the arch running east-west under Puget Sound. P-to-S receiver function analyses and off-shore reflection profiles are consistent with the arch geometry. Another important tectonic feature is the rapid uplift of the Olympic Mountains, which are a horseshoe-shaped post-Eocene accretionary prism. This unusually wide and deep accretionary wedge extends 200 km from the deformation front, but is confined to less than 100 km along arc. To the north and south the prism is much smaller. All these observations seem to be related directly or indirectly to the  $35^\circ$  concave oceanward bend of the trench adjacent to the Olympic Peninsula. Qualitatively, the subduction process forces an initially spherical shell of oceanic lithosphere to pass through the trench, whose curvature is backwards relative to most 'island arcs', and into the mantle. Even though the descending slab retains much of the strength it had as a 'tectonic plate', it must deform to obtain the observed slab geometry.

In order to quantify the relationships among slab geometry, internal deformation, and a variety of geophysical observations, we have concentrated efforts during the past year on the theoretical formulation and implementation of a finite element scheme to invert for both the geometry of a thin sheet (the slab) and the flow field within that sheet which minimizes the global dissipation power associated with its membrane (in-plane)

deformation rate. The sheet is assumed to be a fluid with a Newtonian or a power-law rheology, and an effective viscosity that is at least a few orders of magnitude higher than that of the surrounding mantle. The boundary conditions used for Cascadia subduction are that (1) seaward of the trench, the sheet is a spherical shell rotating at the Juan de Fuca/North America relative plate rates, and (2) the slab dips  $20^\circ$  into the mantle along two cross sections under northernmost California and under northernmost Vancouver Island. The geometry and flow field are otherwise free to vary except that the flow must be in the plane of the slab.

The important aspect of the fixed part of the geometry is the concave oceanward bend in the trench axis which occurs at the latitude of the Olympic Mountains and Puget Sound. The combination of the bend in the trench and the downward dipping slab produce the problem, similar to that of a table cloth hanging over the corner of a table, that there is too much slab material for the available space. The trench geometry forces along-arc compression of the slab, or geometric arching/buckling, or a combination of the two. To obtain a better understanding of this process we perform two calculations: For the first we fix the geometry so that the slab dips at  $20^\circ$  along all cross sections, and invert for the flow field that minimizes global dissipation power for a linear rheology. In the second, we allow the geometry to vary except for a fixed dip of  $20^\circ$  under northern California and Vancouver Island. Figures 2 and 3 show the results of these experiments. In each case, we see along-arc compression (thick line segments) and down-dip extension (thin line segments) landward of the trench. However, the arch geometry results in a strain-rate field that is reduced by a factor of 4 relative to the constant dip model. After inversion for the preferred geometry and strain-rate field the slab displays a pronounced arch (Figure 4, a and b) whose axis is normal to the trench and dips at  $12^\circ$  under the Olympic Mountains and Puget Sound. The arch is flanked by parallel troughs. This minimum strain-rate geometry is similar to the slab geometry estimated by hypocenter distributions and receiver function analyses. In particular, the receiver function study of

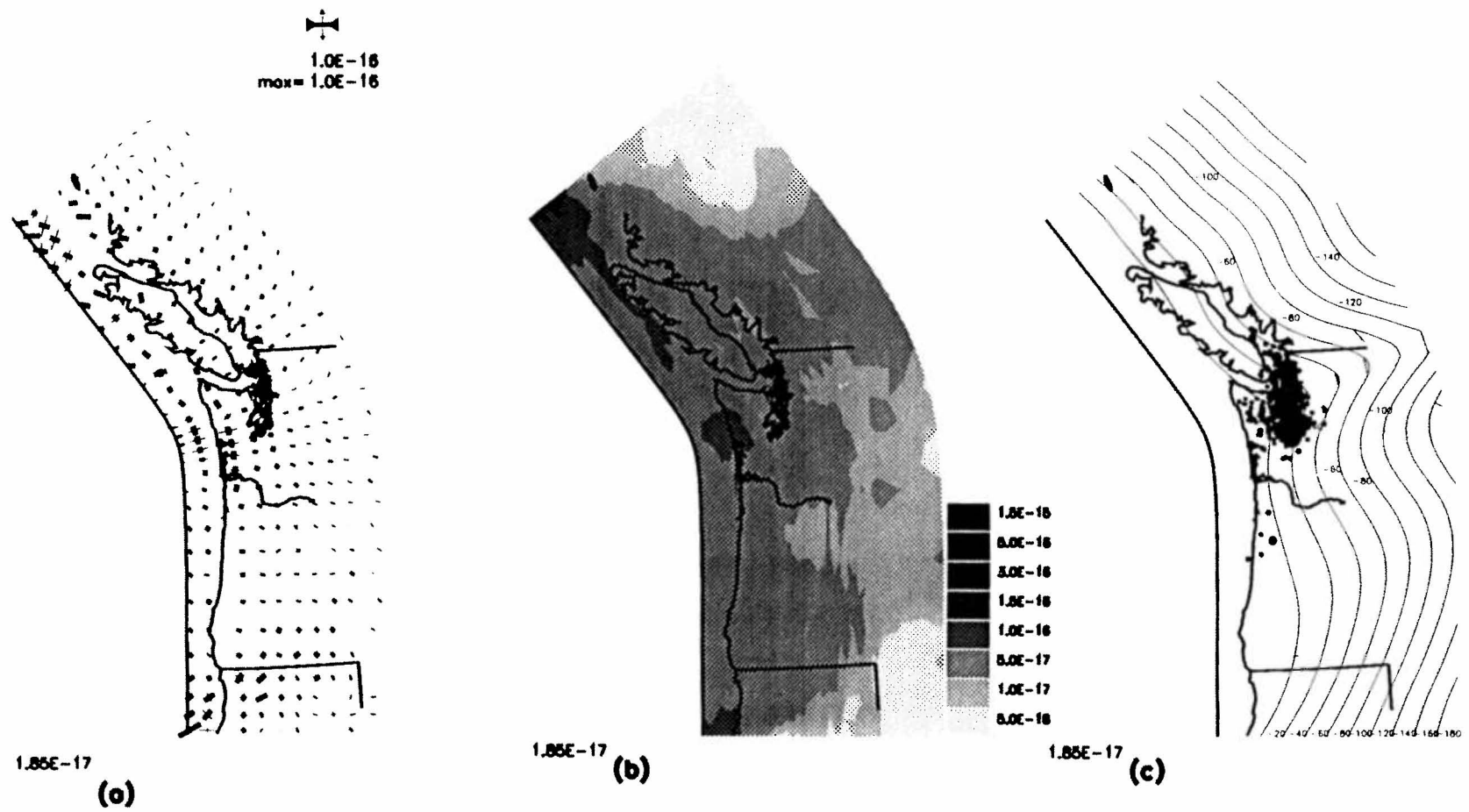


Figure 3. In-Plane strain-rate field resulting from inversion for flow field and slab geometry with slab dip fixed at  $20^\circ$  along the northern and southern edges of the model. Display format is same as Figure 2. Note the reduction of deformation, and the concentration of along-arc compression near the arch axis compared with Figure 2.

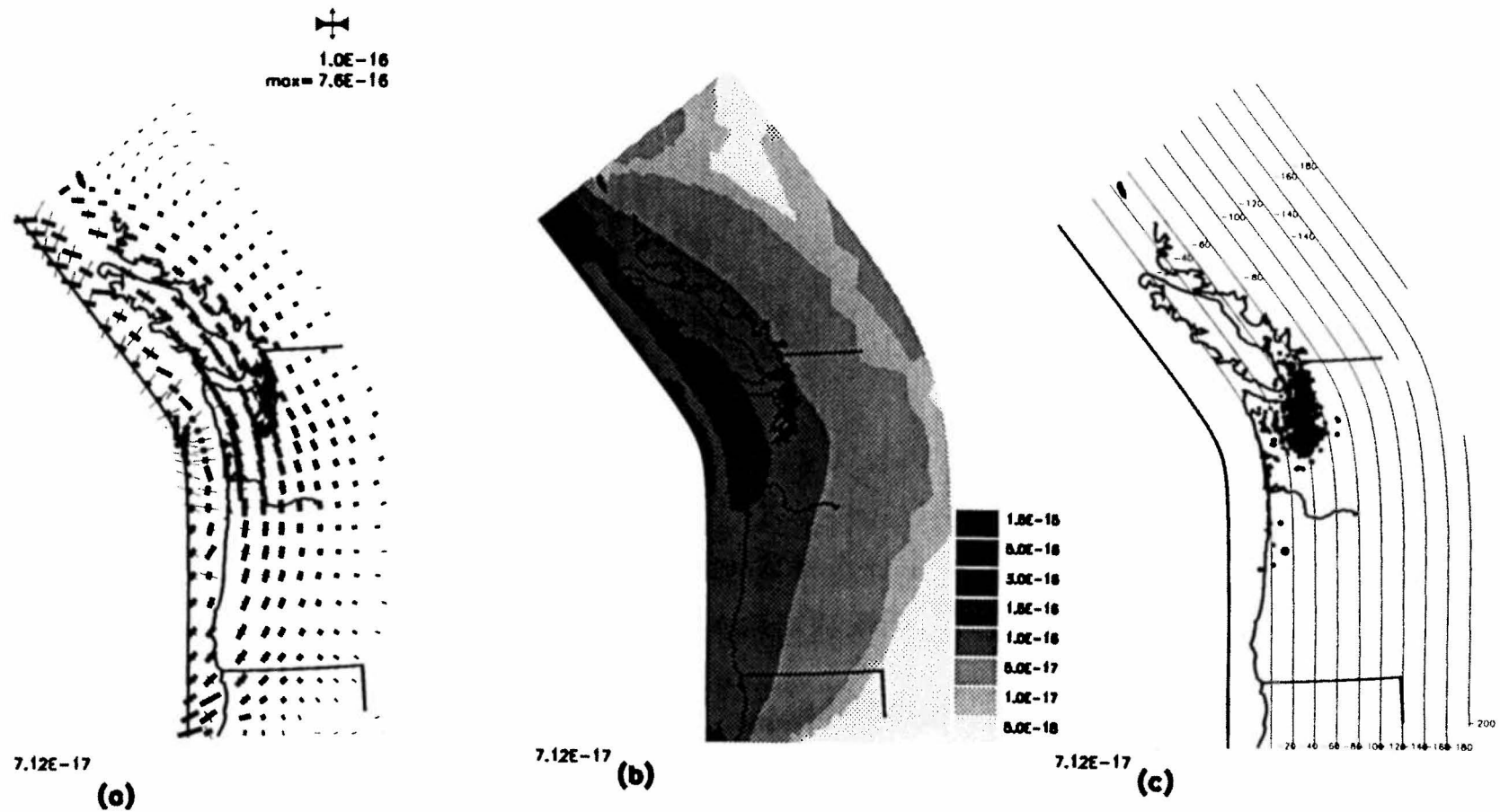


Figure 2. In-Plane strain-rate field resulting from inversion for flow field with geometry fixed at a constant,  $20^\circ$  dip. Solid lines show coastlines, state boundaries and the trench. (a).Orientations of in-plane strain rate showing compressional axes (thick line segments) and extensional axes (thin line segments). Line length is proportional to strain-rate magnitude and saturates at the size and value shown in the key. Units are  $s^{-1}$ . Maximum and root-mean-square effective strain rates are  $7.6 \times 10^{-16}$  and  $7.1 \times 10^{-17} s^{-1}$ . (b). Gray shades showing effective strain rate ( $s^{-1}$ ). (c).Depth contours of the model slab geometry and seismicity occurring within the subducted plate.

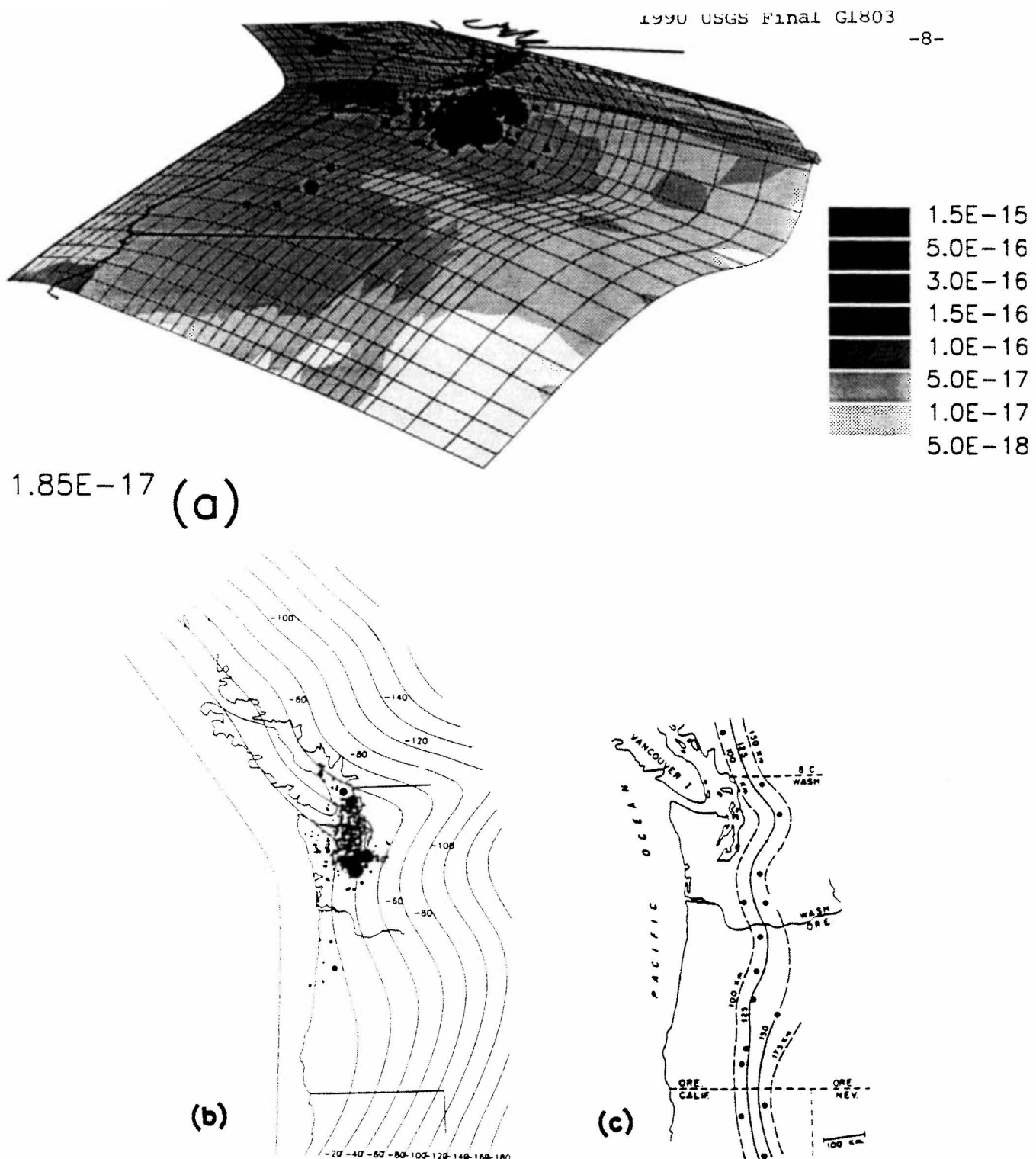


Figure 4. (a).Perspective view of the inverted arch model shown in Figure 3. b and c compare this model with the trend of the volcanic line discussed by Dickinson (1970).

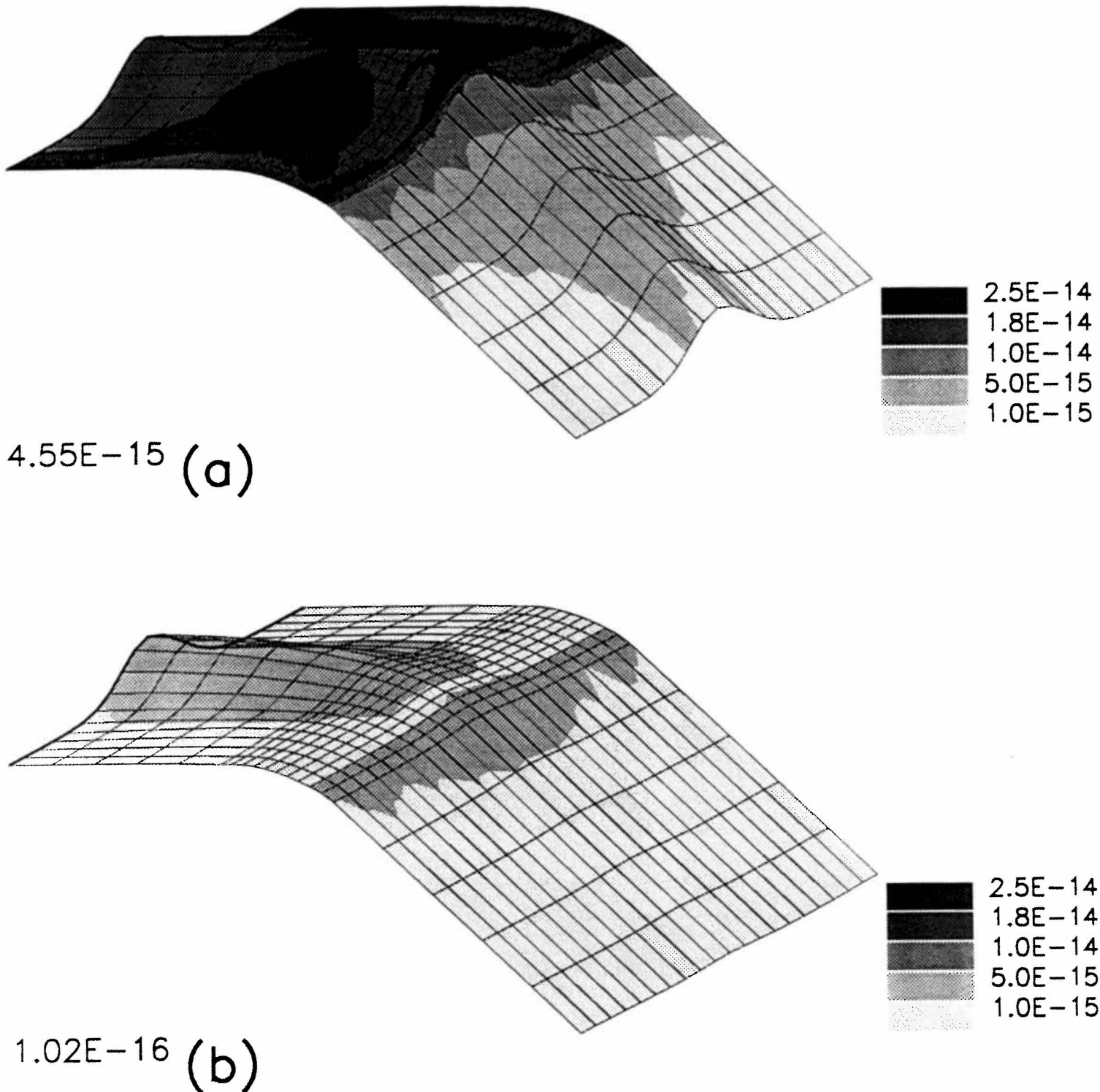


Figure 5. Effect of bending a gaussian shaped arch. (a). Shaded pattern shows the distribution of the effective strain rate when the model geometry is fixed and inversion is performed on the flow field only. (b).Result of a complete inversion by adjusting both the flow field and the model geometry with the gaussian shape fixed at the upper left (solid line) and the dip fixed along near and far edges. The root-mean square effective strain rate is reduced by a factor of 40 when the arch is allowed to relax prior to bending.

Crosson and Owens(1987), and Lapp et al. (1990) suggest that the arch has a tight curvature, and the same dip as that shown in Figure 4. Also, the troughs along the side of the arch are features that, though not yet directly observed, are suggested by leveling data along the Oregon coast (Vincent et al., 1990) and the geometry of volcanic centers (Dickinson, 1970, Figure 4c).

The geometry shown in Figure 4 does not match the observed geometry in one important respect. Tomographic inversion of the deep structure of the slab described in this report provides compelling evidence that the slab below a depth of 100-150 km is dipping steeply, at about 50°. Enormous membrane strains are required to bend the slab to a steeper dip along an axis that is normal to the axis of the arch. This is analogous to bending a sheet of corrugated metal along an axis normal to the corrugations. To quantify this intuitive picture in a calculation that is self consistent with our flow of a sheet of stiff Newtonian fluid, we construct an arch whose shape is gaussian, and bend it by 45°. For this fixed geometry, and a flow field fixed to be parallel to the arch axis as it enters the sheet from the upper left of the diagram, we invert for the flow field within the sheet that minimizes the total dissipation power (Figure 5a). Using this geometry and flow as a starting condition, we fix the geometry along the left, near and far edges as shown in Figure 5b and invert for the flow field and the geometry in the interior of the sheet. The problem in Figure 5a is that it is difficult to bend an arch without large membrane strain rates. The solution (Figure 5b) is to reduce the height of the arch prior to bending it. This new geometry allows the root-mean-squared effective strain rate to be reduced by a factor of 40. The strain rates are highest along the arch. Bending the arch of Figure 4 provides a possible explanation for the observed pronounced concentration of intra-plate seismicity beneath the Puget Sound basin relative to regions to the north or south. Investigations of this hypothesis are continuing.

## Publications funded under this grant

### *Articles*

- Boyd, T.M., and K.C. Creager, 1991, The geometry of Aleutian subduction: Three-dimensional seismic imaging, JGR, V. 96, pp. 2267-2291.
- Creager, K.C. and T.M. Boyd, 1991, The geometry of Aleutian subduction: Three-dimensional kinematic flow modeling, JGR, V. 96, pp. 2293-2307.
- Lees, J.M. and R.S. Crosson, (in press), Bayesian ART versus conjugate gradient methods in tomographic seismic imaging: An application at Mount St. Helens, Washington, AMS-SIAM: Conference on spatial statistics and imaging - June, 1988.
- Lees, J.M. and J.C. VanDecar, 1991, Seismic tomography constrained by Bouguer gravity anomalies, with application to western Washington, PAGEoph., V. 135, pp. 31-52.
- Ma, Li, R.S. Crosson, and R.S. Ludwin, (submitted), Preliminary Report on Focal Mechanisms and stress in western Washington, in: USGS Professional Paper "Assessing and Reducing Earthquake Hazards in the Pacific Northwest")
- Mundal, I., M. Ukawa, and R.S. Crosson, 1991 (in press), Normal and anomalous P phases from local earthquakes, and slab structure of the Cascadia Subduction zone, BSSA

### *Abstracts*

- Chiao, L.Y., and K.C. Creager, 1990, Geometric Constraints of Cascadia Subduction, EOS, V. 71, N. 41, p. 1574.
- Mundal, I., M. Ukawa, and R.S. Crosson, 1990, Evidence of subducting Juan de Fuca plate in apparent velocities observed from subcrustal earthquakes, EOS, Vol. 71, No. 36, p. 1067.
- VanDecar, J.C., R.S. Crosson, and K.C. Creager, 1990, Deep three-dimensional velocity structure of the Cascadia subduction zone, EOS, V. 71, N. 41, p. 1462.
- VanDecar, J.C., R.S. Crosson, and K.C. Creager, 1990, Deep three-dimensional velocity structure of the Cascadia subduction zone, EOS, V. 71, N. 36, p. 1144.
- VanDecar, J.C., R.S. Crosson, and K.C. Creager, extended abstract(in press), Teleseismic travel-time inversion for Cascadia subduction zone structure employing three-dimensional ray tracing, presented at the XXII General Assembly, European Seismological Commission, Barcelona, Spain, Fall, 1990.
- Vandecar, J.C., R.S. Crosson, and K.C. Creager, 1991 (in press) Inferences on the tectonic evolution of deep Cascadia subduction zone structure, for 1991 Vienna IUGG meeting

### Acknowledgements

Work under this grant could not be carried out without the data collected by the Washington Regional Seismographic Network, and we recognize the contribution of the electronic technicians, data analysts, and seismologists of the WRSN.

### References

- Crosson, R.S. and T.J. Owens, 1987, Slab geometry of the Cascadia subduction zone beneath Washington from earthquake hypocenters and teleseismic converted waves, Geophys. Res. Letts., V. 14, pp. 824-827.
- Dickinson, W.R., 1970, Relations of andesites, granites, and derivative sandstones to arc-trench tectonics, Rev. Geophys., V. 8, pp. 813-860.
- Lapp, D.B., T.J. Owens, and R.S. Crosson, 1990, P-waveform analysis for local subduction geometry south of Puget Sound, Washington, Pageoph., V. 133, pp. 349-365.
- Vincent, P., M.A. Richards, and R.J. Weldon, (submitted), Vertical interseismic deformation of the Oregon Cascadia margin J. Geophys. Res.